

Observations of Kuroshio Upwelling from Satellite and Ship Data in the Southern East China Sea

Chen-Te Tseng^{1,2*}, Chi-Lu Sun², Su-Zan Yeh², Shih-Chin Chen¹,
Don-Chung Liu³ and Wei-Cheng Su³

¹Planning and Information Division, Fisheries Research Institute

²Institute of Oceanography, National Taiwan University

³Fisheries Research Institute

ABSTRACT

The quasi-synoptic data obtained from NOAA/AVHRR sea surface temperature (SST) imageries, OrbView-2/SeaWiFS ocean color imageries, and in-situ hydrographic data were applied to investigate the spatio-temporal distribution, of Kuroshio subsurface water and its associated the form of upwelling region (cold eddy) in the summertime. Analyses of the successive AVHRR and SeaWiFS satellite imageries concluded that the corresponding hydrographic patterns and magnitudes of the satellite-derived cold eddy distributions showed a remarkable coincident with ship-observed data. Surface chlorophyll *a* concentrations from SeaWiFS imageries ranged between 0.61 and 1.31 mg/m³ with higher in the Kuroshio upwelling water than in the vicinity. The sea surface temperature gradient from AVHRR imageries in the Kuroshio upwelling region ranged from 19 to 21 °C. The maximum chlorophyll *a* concentration of all hydrographic surveys was 1.99 mg/m³ at 35 m depth and occurred in the Kuroshio upwelling region west of the Pengchiayu Island. The subsurface chlorophyll maximum (SCM) layers were between 10 and 60 m in the southern East China Sea. However, the SCM was shallower than 30 m and usually extended to the sea surface in the Kuroshio upwelling region. Therefore, the multi-sensors imageries derived from the SeaWiFS ocean color and AVHRR SST data can be a powerful tool to identify some important hydrographic patterns, ex. the Kuroshio upwelling, and cold eddy.

Key words: Kuroshio upwelling, cold eddy, sea surface temperature, ocean color

INTRODUCTION

The East China Sea with an extensive continental shelf region is a large marginal sea in the western Pacific Ocean. The shelf of the East China Sea receives a large amount of dissolved inorganic nutrients and sediments originating from the freshwater of the Changjiang and other rivers, and the upwelling of Kuroshio subsurface and near-bottom

waters (Shen *et al.*, 1993; Gong *et al.*, 2000; Wong *et al.*, 2000; Hung *et al.*, 2003; Shi *et al.*, 2004). The shelf off southern East China Sea is also a region of interaction among the Taiwan Warm Current, the Kuroshio Current, the Mainland coastal water, and the East China Sea shelf water. The exchange rate of sedimentary substance between the southern East China Sea shelf water and the Kuroshio waters is estimated to be about 4.68×10^8 metric tons per year (Li and Chen, 1998), indicating that the chemistry of the continental shelf water in northeastern Taiwan was mostly influenced by the Kuroshio inputs (Li, 1994). Cold eddies associated with the Kuroshio

*Correspondence: 199 Hou-Ih Road, Keelung 202, Taiwan. TEL: (02) 2462-2101; FAX: (02) 2462-4627; e-mail: ctseng@mail.tfrin.gov.tw

upwelling in the southern East China Sea had been reported by several authors using in situ CTD and ADCP data (Liu *et al.*, 1992; Tang and Tang, 1994; Sun and Xiu, 1997; Tang *et al.*, 2000), Physical-Chemical data (Wong and Zhang, 2003; Wong *et al.*, 2004) and satellite thermal infrared imageries (Lin *et al.*, 1992; Tseng *et al.*, 2000; Liu *et al.*, 2004). In formation of high primary productivity region, it requires adequate nutrient replenishment for photosynthetic process of marine phytoplankton. Therefore, the Kuroshio upwelling waters should provide the dominant source of nutrient-rich water in the southern East China Sea. However, the temporal and spatial variations of Kuroshio upwelling water are usually associated with the location of the Kuroshio Current. Generally, the Kuroshio moves close to and sometimes onto the shelf during wintertime and offshore in summertime off northeastern Taiwan (Sun, 1987; Tang *et al.*, 2000). As a result, the upwelling phenomenon is found usually and normally related to the Kuroshio subsurface or near-bottom water in summer.

The chlorophyll a (hereafter Chl-a) has been regarded as an important index for the estimation of phytoplankton biomass and primary productivity (Bukata *et al.*, 1995). High Chl-a concentration areas are usually good fishing grounds, supporting large commercial fisheries (Larus *et al.*, 1984; Fiedler and Bernard, 1987). Recent development of satellite ocean color remote sensing and the observation of temporal and spatial variability of the spring bloom over broad synoptic scales has provided a unique tool for the study of these features (Saitoh *et al.*, 1998). Cold and nutrient-rich upwelling water is an important indicator for local primary productivity and fishery resources (Lohrenz *et al.*, 1999; Rodriguez *et al.*, 1999; Hardman-Mountford *et al.*, 2003). With the help of the SeaWiFS sensor boarded on OrbView-2 satellite, inheriting after the Nimbus/CZCS (1978-1986) and ADEOS/OCTS (1995-1996), ocean color can be measured to estimate the Chl-a concentration over sea surface. In addition, the NOAA/AVHRR sea surface temperature imageries can reveal the water mass distribution. Ning *et al.* (1998) concluded that the ocean color and infrared imageries complement each

other because a useful tool for interpretation of the spatial and monthly variations of the circulation patterns in the East China Sea. Since upwelling region changes rapidly, study of the spatial distributions of upwelling and associated phytoplankton variations is difficult by ship surveys. Therefore, satellites remote sensing is the only tool currently available for instantaneously observation of the spatial distribution of regional upwelling as well as the larger scale ocean patterns. The intrusion of Kuroshio subsurface water over the continental shelf off northeastern Taiwan and its interaction with the coastal and mixed water of East China Sea to form fronts or upwelling eddies had been reported mainly by ship observations. So the satellites NOAA/AVHRR sea surface temperature, OrbView-2/SeaWiFS ocean color imageries, and in situ hydrographic data are used in this study to examine the presence of Kuroshio upwelling in the southern East China Sea. Additionally, the objectives of this study also would like to confirm the utilities of satellite remote sensing data in exploring the important oceanographic features, especially cold eddies.

MATERIALS AND METHODS

1. Satellite imageries

The ocean color imageries were geometrically processed from SeaWiFS (Sea-viewing Wide Field-of-view Sensor) level-1A data of OrbView-2 satellite provided by the Tokai University Information Technology Center (TRIC) in Tokyo, Japan. The satellite imagery of 1.1x1.1 km² resolution (IFOV at nadir) represents the averaged Chl-a concentration (mg/m³) of the upper ocean. The sea surface temperature imageries were derived from AVHRR (Advanced Very High Resolution Radiometer) data archived by the NOAA/HRPT (High Resolution Picture Transmission) station of the Satellite Remote Sensing Laboratory in FRI (Fisheries Research Institute) in Keelung, Taiwan. The AVHRR on board the NOAA polar orbiting satellite was equipped with a five-channel sensor in visible and infrared wavebands. The raw HRPT

telemetry data are used to construct digital SST imageries using the Multi-Channel Sea Surface Temperature (MCSST) method (McClain *et al.*, 1985; SeaSpace, 1992). Those SST imageries were also of $1.1 \times 1.1 \text{ km}^2$ resolution (IFOV at nadir).

2. In-situ hydrographic data

The two synoptic and intensive hydrographic surveys were conducted over the shelf area off southern East China Sea CR-9808 (August 25-27, 1998) by the R/V “*Ocean Researcher 2*” and CR-0507 (July 13-16, 2005) by the R/V “*Hai-Chien*”. The hydrographic stations of two cruises and topography in the vicinity of the study area are shown in Fig. 1. The cruises track crossed over one valley, the Keelung Valley and two canyons, the Mienhwa and North Mienhwa Canyon. In CR-9808 cruise (upper panel of Fig. 1), a total of 31 CTD stations, labeled A1 to A35 along four transect lines X1 (A2-A8), X2 (A10-A17), X3 (A19-A26) and X4 (A28-A35), formed a similar rectangle, and in CR-0507 cruise (lower panel of Fig. 1), there are 33 CTD stations, labeled B1 to B33 (including transect line A (B2-B29) and B (B1-B33)). CTD data (Model SBE9/11 Plus, Sea Bird Electronics, USA) are collected to obtain vertical profiles of water temperature ($^{\circ}\text{C}$), salinity (psu) at different depths. Vertical profiles of Chl-a (mg/m^3) concentration were determined with a Sea Tech fluorometer attached to the CTD in CR-9808 cruise. The current velocity was obtained from a shipboard Acoustic Doppler Current Profiler (Sb-ADCP) in CR-9808 cruise, and the U-components (eastward) and V-components (northward), and flow velocity (cm/sec) and direction were measured.

RESULTS AND DISCUSSION

1. Water masses in the southern East China Sea

The water temperature, salinity, density and Chl-a concentration from oceanographic CTD surveys of the cruises CR-9808 and CR-0507 were

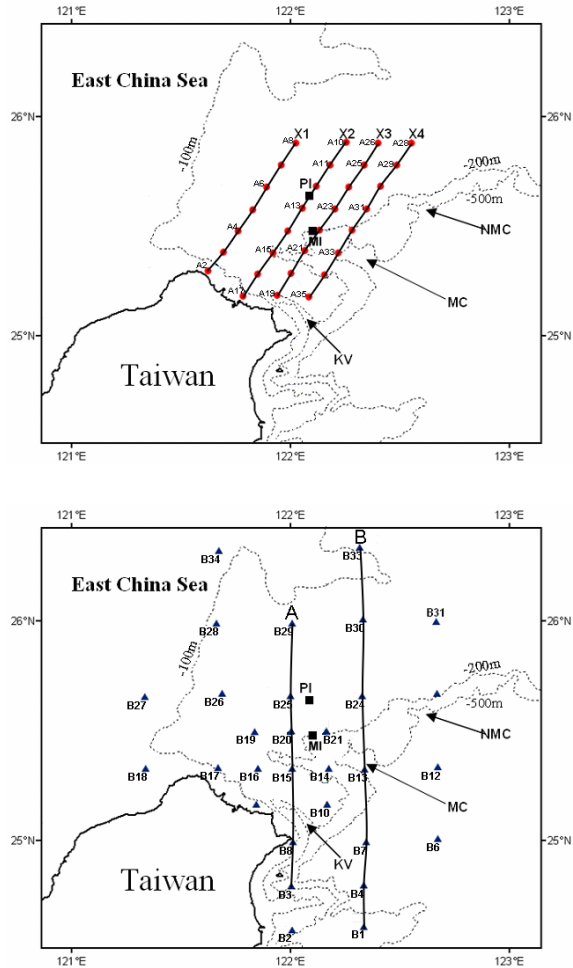


Fig. 1 Geographical locations of the CR-9808 cruise (upper panel), August 25-27, 1998 (solid circles, transect X1 (A2-A8 stations), X2 (A10-A17 stations), X3 (A19-A26 stations), X4 (A28-A35 stations)) and the CR-0507 cruise (lower panel), July 13-16, 2005 (triangle circles, transect A (B2-B29 stations), B (B1-B33 stations)) hydrographic survey stations. The isobaths of topography are indicated by dashed lines. Abbreviations are geographic name referred to in this paper: PI=Pengchiayu Island; MI=Mienhuayu Island; NMC=North Mienhwa Canyon; MC=Mienhwa Canyon; KV=Keelung Valley.

used to examine the intrusion of Kuroshio surface and subsurface water. In this study, three different water masses could be discriminated from the T-S diagrams (Fig. 2): the coastal shelf water (Type-1), the Kuroshio upwelling water (Type-2), and the Kuroshio water (Type-3) in the southern East China Sea. Hur *et al.* (1999) had used long-term historical temperature and salinity observations to investigate

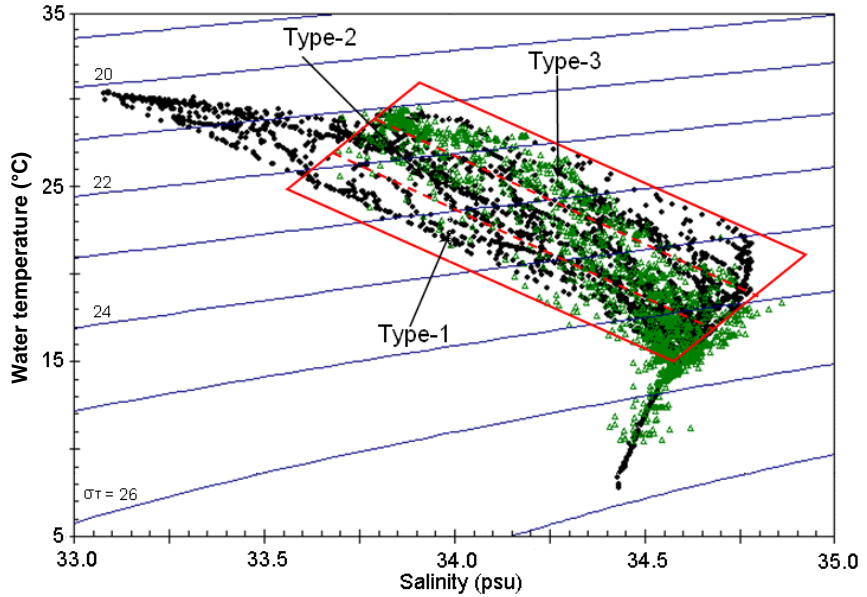


Fig. 2 T-S diagrams of all CTD sampling data from CR-9808 and CR-0507 cruises in the southern East China Sea. Three different water masses could be discriminated from the T-S diagrams: the coastal shelf water (Type-1), the Kuroshio upwelling water (Type-2), and the Kuroshio water (Type-3).

found that the major masses included Kuroshio-East China Sea water, mixed water, and the coastal water. The present study showed that the coastal shelf water nearby the northeastern coast of Taiwan was cooler and less salty. The Kuroshio upwelling water was around the Pengchiayu Island and could follow the intrusion path of the Kuroshio subsurface water along the Mienhwa Canyon. Hsueh (2000) concludes that south of about 28° N, the Kuroshio runs into the continental shelf and is uplifted. The third type was warm and salty Kuroshio water at the northern stations of the four transect-lines. The influence of coastal water and northern East China Sea mixed water was usually weak in summer; the dominant hydrographic feature was the cold eddy derived from Kuroshio upwelling.

The vertical profiles of water temperature and salinity of three different water-masses at the CTD stations of A3, A13 and A28 were shown as Fig. 3. The coastal shelf water (A3) displayed three water layers in summer. Both the thermocline and halocline layers were found at about 20~25 m and 45 ~ 60 m deep. The surface water layer is the coastal water, and the salty water (below 60 m) is the Kuroshio water. These two water masses formed the mixed water at 20~50 m depths. In contrast, water was well mixed from the bottom to the surface in the Kuroshio upwelling region (A13 in Fig. 3). Water temperature

decreased gradually and salinity increased slowly down to the bottom layer. In the Kuroshio region (A28), the thickness of the mixed layer ranged between 20 and 35 m in the salinity profile. The upper water is the coastal water and the near-bottom water was similar to the Kuroshio salty water. The well mixed surface water in the Kuroshio region is a result of solar radiant heating; a shallow mixed layer (thickness < 20 m) is usually observed in Kuroshio water in summer (Gong *et al.*, 1999)

2. Detection of Kuroshio upwelling region derived from AVHRR data

In this study, the NOAA/AVHRR sea surface temperature imageries and OrbView-2/SeaWiFS ocean color imageries had shown a dominant cold eddy surrounded by warmer water (higher than 30 °C) close to the Pengchiayu Island in August 26-27, 1998 and July 16, 2005 (A1-A3 of Fig. 4). Generally, the lower water temperature, the stronger the SST gradient, is representing a highly mature stage of the cold eddy. The first SST image of August 26, showed a cold eddy near A13 station of CR-9808 cruise, about 8.1 km from the Pengchiayu Island and Mianhuayu Island. The lowest sea surface temperature was about 25.4 °C, close to the lowest temperature in the cold eddy and could be used to

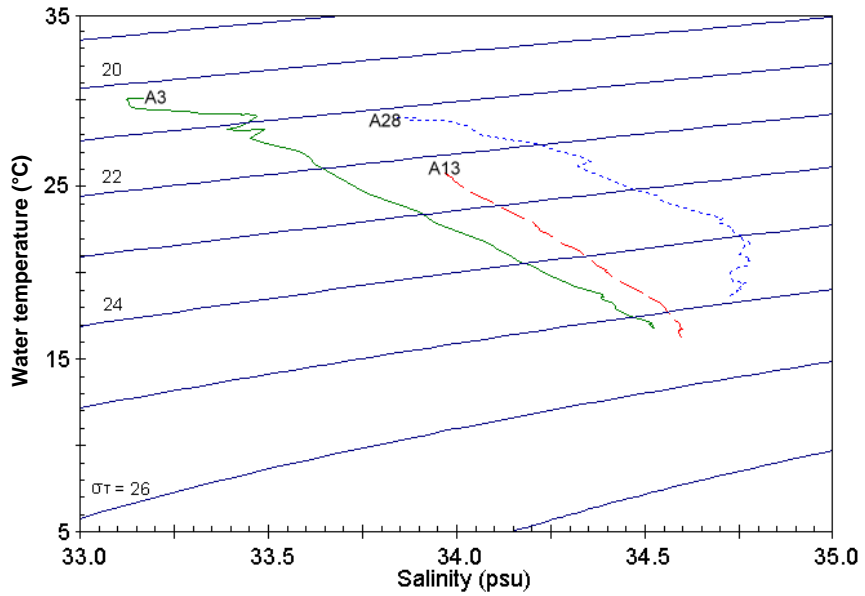


Fig. 3 Vertical profiles of water temperature and salinity of three typical water masses were represented from the CTD stations: A3 (the coastal water), A13 (Kuroshio upwelling water), and A28 (Kuroshio mainstream water).

Table 1 The characteristics and measures of a progressive cold eddy observed from successive NOAA/AVHRR SST imageries

Date	1998/8/25	1998/8/26	1998/8/27
Satellite	NOAA-12	NOAA-12	NOAA-14
Observed Time	17:49 CST	17:25 CST	14:15 CST
Coldest Center	25.523° N 122.108° E	25.587° N 122.070° E	25.669° N 122.029° E
Lowest Temperature	25.4 °C	25.4 °C	26.2 °C
Area within 29 °C isotherm	2600 km ²	2300 km ²	1800 km ²
Area within 28 °C isotherm	1100 km ²	1000 km ²	800 km ²

exhibit the developed stage of the cold eddy. On August 27, the center of cold eddy moved northwestward to A12 station, about 9.9 km from the Pengchiayu Island. The maximum temperature increased to about 26.2 °C and the region decreased to about 1800 km² (bounded by 29 °C isotherm), implied that the cold eddy decayed slowly (Table 1). From August 25 to 27, the Kuroshio water intruded onto the continental shelf along the Mienhwa Canyon to form an eddy on August 26. Thus, the movement of cold eddy could indicate the variation of the intrusion of the Kuroshio subsurface water.

In addition, the similar cold eddy was also found from another associated satellite imageries of AVHRR sea surface temperature image on July 16, 2005 in CR-0507 cruise (A3 of Fig. 4). In the

southern East China Sea, the Kuroshio upwelling phenomenon has been found from many multi-sensor satellite imageries and oceanography surveys. The Kuroshio Edge Exchange Processes (KEEP) project, which was initiated in 1989 and completed in 2000, has made significant contribution to the understanding of biogeochemical and hydrodynamic processes in the southern East China Sea. The hydrographic surveys of KEEP project have confirmed the year-round existence of the topography induced upwelling of Kuroshio subsurface water near the southern East China Sea. Therefore, the remarkable cold eddies induced by intrusion of Kuroshio upwelling water usually with cooler sea surface temperature were detected by NOAA/AVHRR satellite imageries.

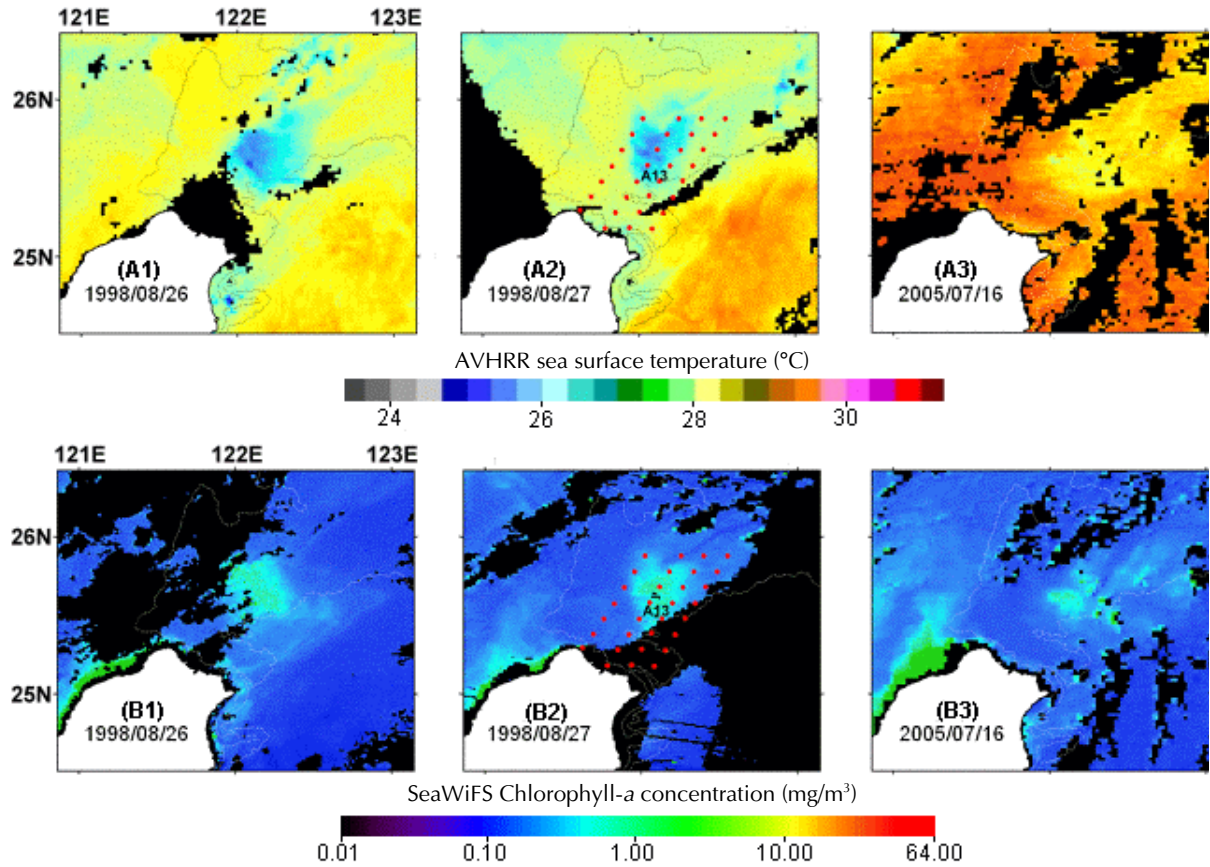


Fig. 4 The corresponding NOAA/AVHRR sea surface temperature imageries (A1-A3) and Orbview-2/SeaWiFS ocean color imageries (B1-B3) during CR-9808 and CR-0507 cruises. Those satellite imageries had shown that the noticeable cold eddies induced by Kuroshio upwelling events.

3. Detection of Kuroshio upwelling region derived from SeaWiFS data

The SeaWiFS ocean color (Chl-a concentration) imageries from August 26-27, 1998 and July 16, 2005, corresponding with AVHRR sea surface temperature imageries covering southern East China Sea had been shown in B1-B3 of Fig. 4. Cold eddies induced by the intrusion of Kuroshio upwelling water was found in both the SeaWiFS ocean color imageries and AVHRR SST imageries. The high Chl-a concentration water was found in the cold eddy region with the Kuroshio upwelling water. The ocean color imageries showed that the Chl-a concentration was lower in the deep water of Kuroshio mainstream region than the upwelling region of southern East China Sea. From those

SeaWiFS imageries, the Chl-a concentration decreases from the upwelling region, the Kuroshio water and to the coastal water. Surface Chl-a concentrations were between 0.61 and 1.31 mg/m³ in the upwelling region, 0.3 to 0.44 mg/m³ in the coastal water shelf, and 0.21 to 0.86 mg/m³ in the Kuroshio water. The results were similar to that described by Chen (2000). The AVHRR and SeaWiFS imageries (Fig. 4) showed that induced cold eddies of Kuroshio upwelling coincided with both SST and ocean color imageries. Most cold eddies located at the offshore off southern East China Sea should be of the Case 1 (oceanic) water. A good correlation was found between SST and Chl-a concentration in the Kuroshio upwelling region. Higher Chl-a concentration was also found in the inshore coastal water, the Case 2 (turbid)

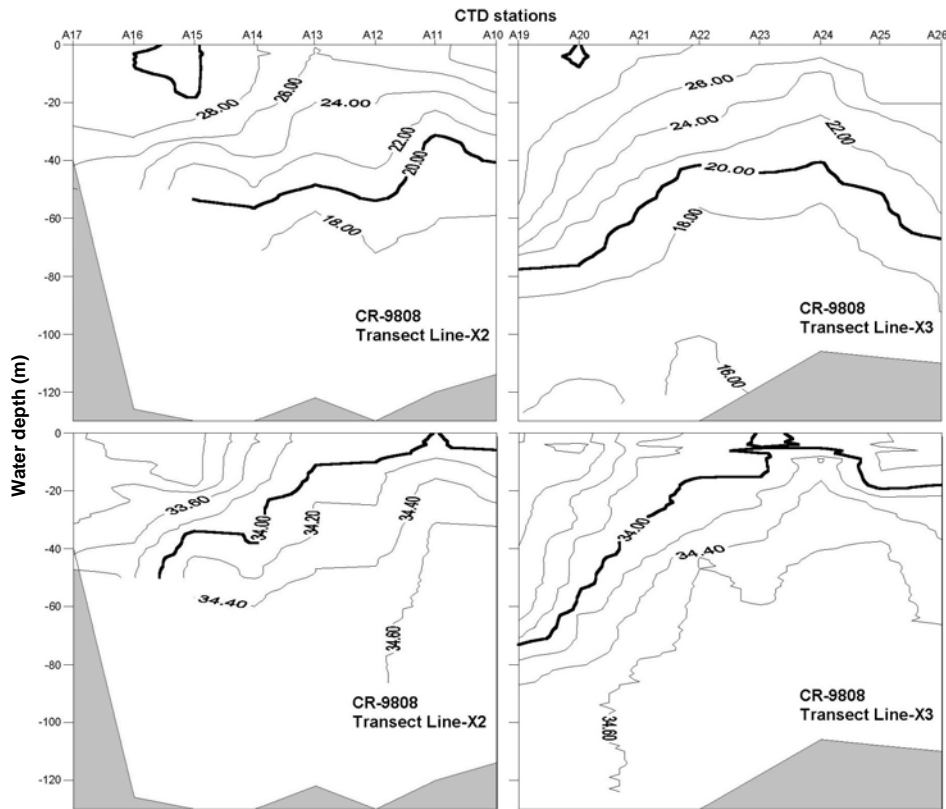


Fig. 5 Vertical cross-sections of water temperature ($^{\circ}\text{C}$, upper panel) and salinity (psu, lower panel) during CR-9808 in the southern East China Sea (transect line X2 & X3 in Fig. 1).

water. Toba and Murakami (1998) suggest that combined use of SST and ocean color imageries could thus reveal oceanic conditions more clearly than the use of SST imageries alone.

Does the Chl-a concentration of phytoplankton population follow the rapid environmental changes during different stages of the upwelling? Service *et al.* (1998) reported that the freshly upwelled water is low in phytoplankton biomass. In the present study, we also found that the older upwelling water had higher surface Chl-a concentration than the freshly upwelled water. Fig. 4-B1 showed a cold eddy with maximum surface Chl-a concentration about 1.49 mg/m^3 in the ocean color image on August 26. In addition, old upwelling water was nutrients-rich, with concentration related to the exposure time in euphotic zone. The phytoplankton biomass in the shelf water was limited by the light variability due to the short exposure time of the upwelled water (Gong *et al.*, 2000). Therefore, upwelled phytoplankton populations may not be

fully acclimatized to their environment, resulting in a time lag between the introduction of the upwelling water to the surface and subsequent phytoplankton blooms (Service *et al.*, 1998). Denman and Abbott (1994) found pigment increases (measured from CZCS imageries) to lag behind temperature decreases (measured from AVHRR imageries) for 1-2 days. So, the maximum Chl-a concentration did not appear at the time of lowest temperature in the cold eddy. Furthermore, the corresponding AVHRR sea surface temperature image and SeaWiFS ocean color image has shown that the Kuroshio upwelling area (cold eddies) usually has a higher Chl-a concentration and cooler sea surface temperature as in summer of 2005 (Fig. 4-A3 & -B3).

4. Hydrographic observations of Kuroshio upwelling region

Figure 5 shows the vertical cross-sections of CTD water temperature and salinity on the southern

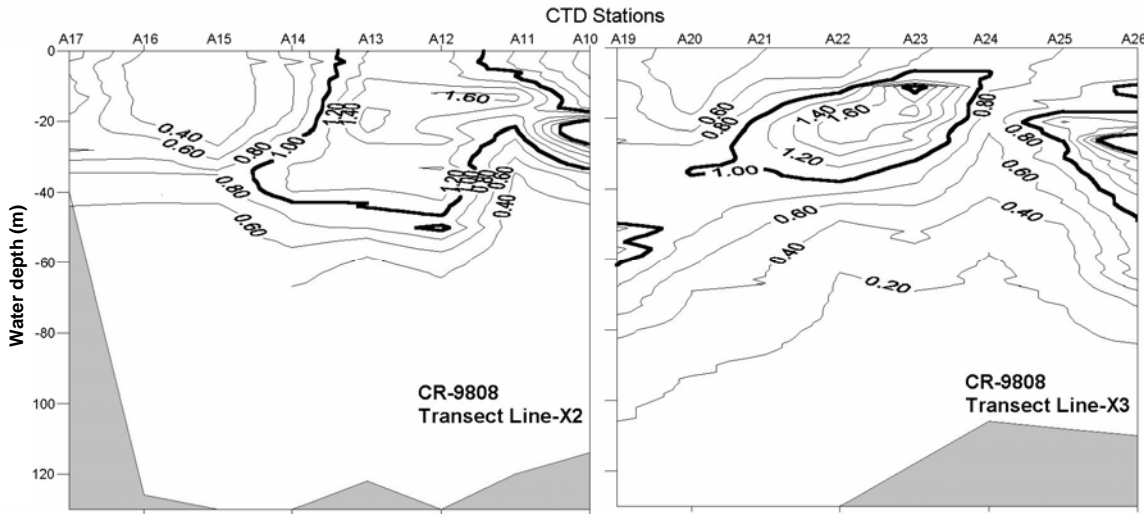


Fig. 6 Vertical cross-sections of chlorophyll a concentration (mg/m^3) during CR-9808 in the southern East China Sea (transect line X2 & X3 in Fig. 1).

shelf of East China Sea (CR-9808 cruise-Transect line X2 & X3 in Fig. 1). It showed that the Kuroshio upwelling was evident as indicated by the upward-tilting isotherms and isohalines. This study had found that the Kuroshio subsurface water intruded onto the East China Sea shelf between A11 to A14 in transect line X2 of CR-9808 cruise (left panel of Fig. 5). Hsueh (2000) also concludes that south of about 28° N , the Kuroshio runs into the continental shelf and is uplifted. It is also found that the area with Chl-a concentration higher than $1.0 \text{ mg}/\text{m}^3$ is always distributed in the subsurface layer, between 10-60m depth of A12 to A13 CTD stations (Fig. 6). Chen (1995) had pointed out that the Kuroshio subsurface water (upwelling water) usually show high apparent oxygen utilization and nutrients with a subsurface chlorophyll maximum (SCM) at a depth from 20 to 60 m in the euphotic zone. In this study, the maximum Chl-a concentration of $1.99 \text{ mg}/\text{m}^3$ in the 35 m depth of A6 (in transect line X1), appeared in the Kuroshio upwelling region off the western Pengchiayu Island. Furthermore, the water above the SCM layer apparently had little nutrient supply for phytoplankton even though there is sufficient light in the surface water. It is believed that the thermocline and halocline layer blocked up the nutrients-rich water. Along the transect line X3 section of CR-9808 cruise (right panel of Fig. 5), the

uplifting isopleths were located around A22 to A25 in the region of the upwelling subsurface water. The higher Chl-a concentration ($> 1.0 \text{ mg}/\text{m}^3$) was at the surface and down to 60 m depth in the Kuroshio upwelling region. In the SCM layer, it was about $1.70 \text{ mg}/\text{m}^3$ in the 20 m depth at A23.

From these two vertical cross sections of transect X2 and X3, we concluded that the Kuroshio upwelling region has been observed in the southern East China Sea. Furthermore, the SCM formation in the subsurface layer was also observed, in depth ranging from 10 to 60 m. However, the SCM was below 30 m depth and extended to the surface in the Kuroshio upwelling region. Chen (2000) reported that the shallow subsurface layer maximized between 0 and 25 m in the Kuroshio upwelling region, in contrast to 50 and 75 m in the Kuroshio water. Generally, due to lack of nutrients in the upper water and lack of light in near-bottom water, the SCM layer usually forms at the subsurface layer beneath the strong thermocline in summer.

Additionally, the Kuroshio fronts were also found in the transect X2 and X3 (Fig. 5 and Fig. 6). At A13 to A14 of transect X2, and A21 to A22 of transect X3, those isopleths of water temperature and salinity had expressed to exist the frontal structures and patterns. The high Chl-a concentration water was always on the right side of the front structure.

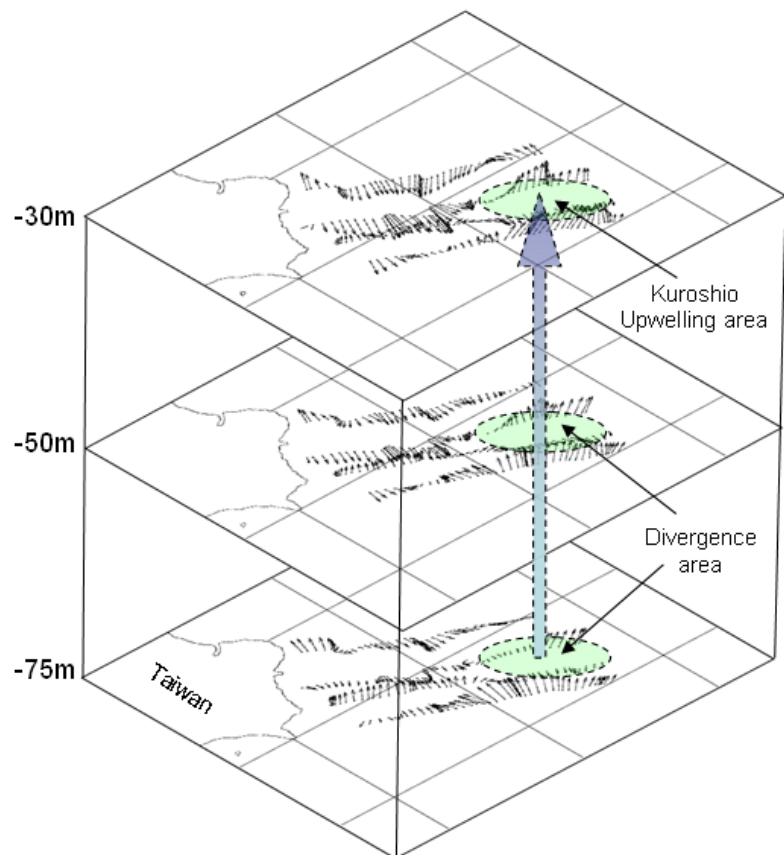


Fig. 7 The 3D diagram of Kuroshio upwelling event from Sb-ADCP current-vector profiles off southern East China Sea during CR-9808 cruise in 1998.

Kuroshio fronts were easily found on the inshore side when the Kuroshio subsurface or near-bottom water intruding onto the shelf northeast of Taiwan. On the offshore side, high Chl-a concentrations were only found in cold eddies of Kuroshio upwelling water. However, the thermocline and front usually exist at the same time in the south of northeastern Taiwan (Yu and Miao, 1990; Chern and Wang, 1994). Therefore, the depth of the variations of thermocline layers and the location of cold eddies and fronts play an important role in the Chl-a concentration and its spatial distribution.

The 3D diagram of Kuroshio upwelling event off southern East China Sea during CR-9808 cruise in 1998 was shown as Fig. 7. From ADCP current vectors analysis of transect line X2 & X3, there is a remarkable convergent area exist in south of latitude 25.5N near northeastern Taiwan. About locations of A13 & A22 CTD stations, north of latitude 25.5 N, a divergent area was found in 75 m depth to surface layer (30 m depth). This upward event from

divergent effect of transect line X2 & X3 had been indicated as the Kuroshio upwelling in this study. The upwelling of Kuroshio subsurface water could contribute colder and richer nitrate water from bottom to the surface layer. Therefore, the cold eddies and high Chl-a concentration regions could be observed from AVHRR and SeaWiFS imageries in the southern East China Sea (Fig. 4).

Figure 8 shows the contours of water temperature and Chl-a concentration in different water layers from all CTD stations of CR-9808 cruise. There is a close relationship between water temperature and Chl-a concentration, higher Chl-a concentration in the cold water and lower Chl-a concentration in the warm water. Cold eddies associated with Kuroshio upwelling were near the Pengchiayu Island with lowest temperature less than 23 °C and maximum Chl-a concentrations higher than 1.0 mg/m³. And the Chl-a concentration is usually uniform from the surface to 30 m depth.

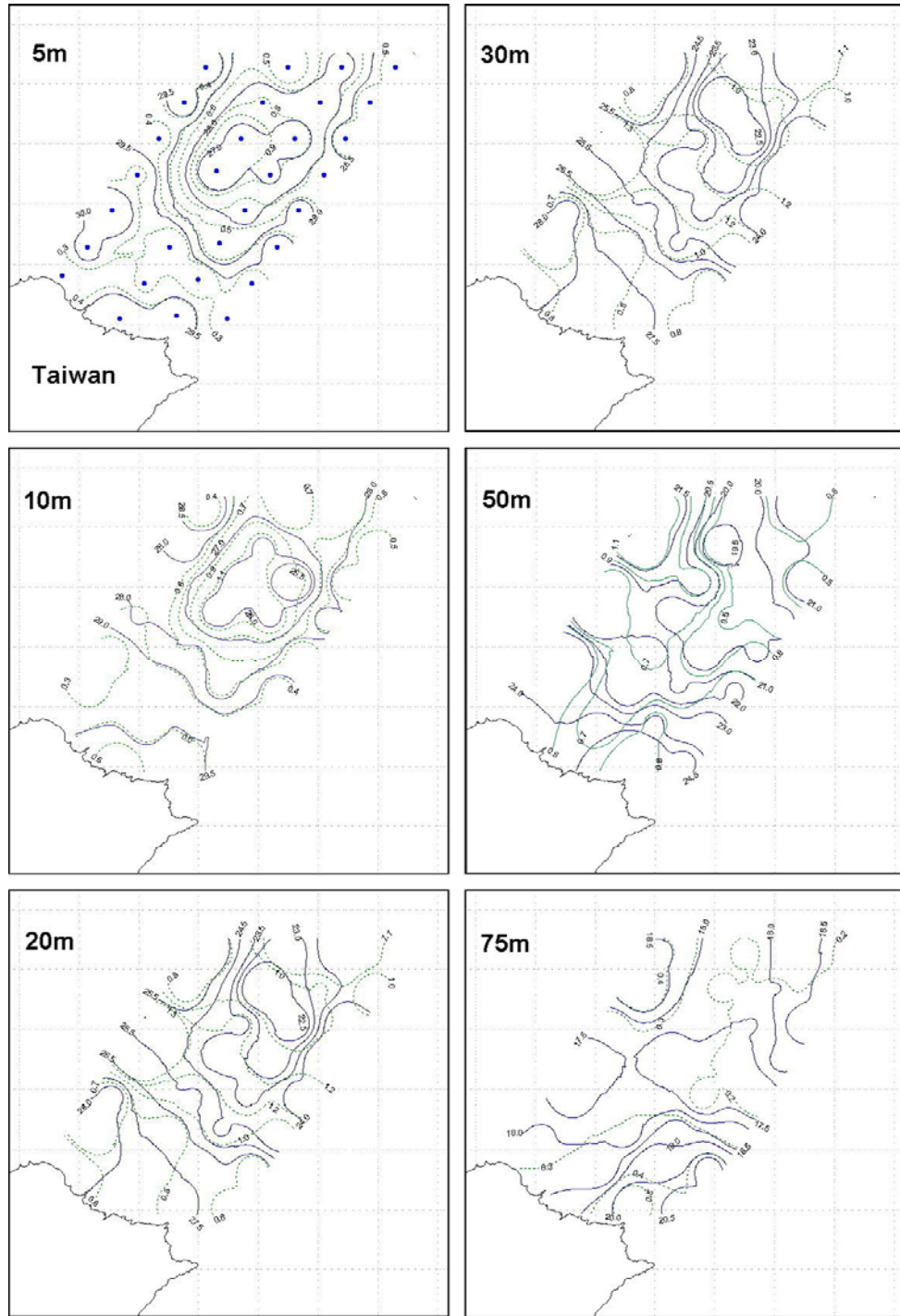


Fig. 8 Joint contours of water temperature ($^{\circ}\text{C}$, solid line) and Chl-a concentration (mg/m^3 , dashed line) in different water layers.

From analysis of CTD data of CR-0507 cruise, the Kuroshio upwelling region has also been found in the southern East China Sea. Fig.9 show the CTD water temperature and salinity profiles of transects line A and B. The upwelling region was found to be

located between B15 to B25 and B7 to B24, respectively. In addition, the corresponding upwelling region has also been observed from AVHRR and SeaWiFS imageries (Fig. 4).

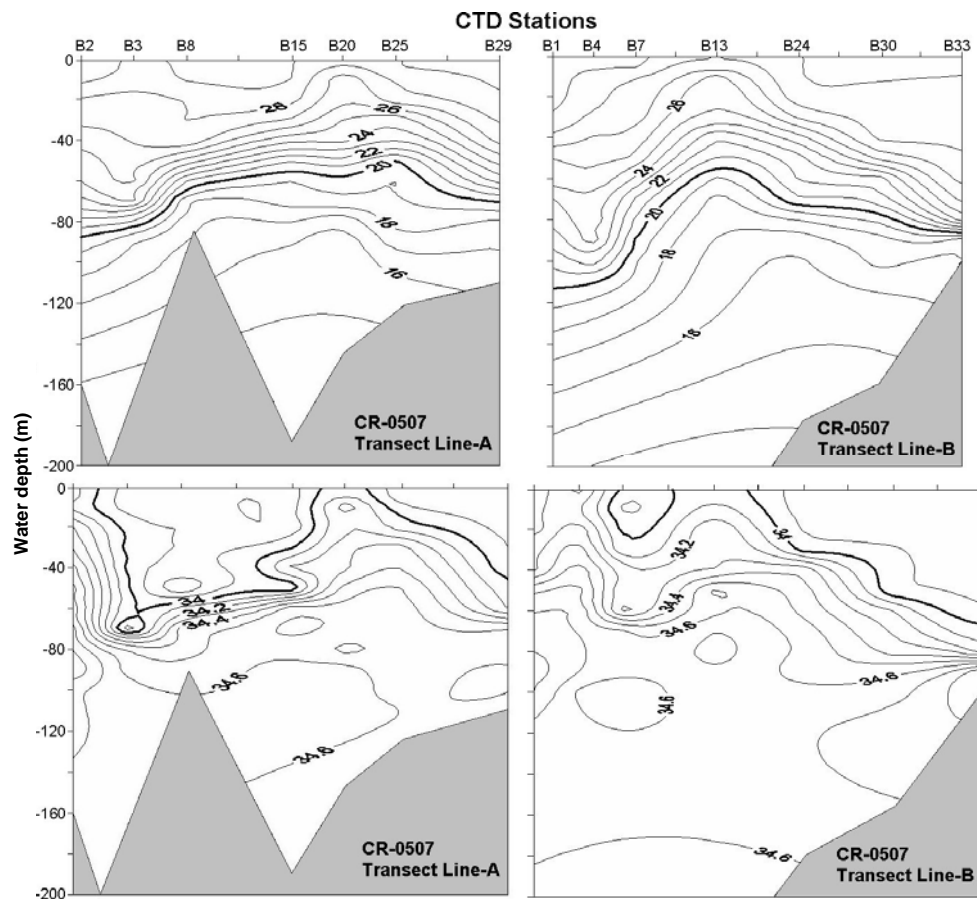


Fig. 9 The CTD water temperature ($^{\circ}$ C), upper panel) and salinity (psu, lower panel) profiles of transect line A and B. The upwelling region was found to locate between B15 to B25 and B7 to B24, respectively.

Conclusions

The Kuroshio water intrusion plays an important role in the formation of cold eddies in the southern East China Sea. The upwelling water could bring nutrients from the Kuroshio subsurface or near-bottom water to the surface, and intensification of the photosynthesis of marine phytoplankton resulting in high Chl-a concentration around the southern shelf of East China Sea. In this study, local Kuroshio upwelling water in the southern East China Sea was evident base on the AVHRR sea surface temperature and SeaWiFS Chl-a concentration. The SeaWiFS-derived Chl-a distributions showed a remarkable coincidence with the ship-observed pigment distributions. The patterns of pigment distributions were also similar to those observed in sea surface temperature. The upwelling region was

frequently observed with high Chl-a concentration and low temperature in sea surface. Cold water implies high primary productivity and warm water implies low primary productivity in this region. In addition, a good relationship existed among the sea surface temperature, the Chl-a concentration, and the depth-averaged Chl-a concentration in the euphotic zone. The combined use of the NOAA/AVHRR sea surface temperature and OrbView-2/SeaWiFS ocean color imageries from multi-platform satellites can be utilized in analysis of physical and biological processes of Kuroshio upwelling in the southern East China Sea.

ACKNOWLEDGEMENTS

The authors wish to appreciate the share of CTD and ADCP data from the National Center for

Ocean Research. We also would like to thank the comments of two anonymous reviewers were most helpful.

REFERENCES

Bukata, R. P., J. H. Jerome, K. Y. Kondratyev and D. V. Pozdnyakov (1995) Optical Properties and Remote Sensing of Inland and Coastal Waters. CRC Press, Inc., Florida, USA, 362pp.

Chen, Y. L. L. (1995) Temporal and spatial changes of chlorophyll *a* in the KEEP study waters off northern Taiwan. *Terrestrial, Atmos. Oceanic Sci.*, 6: 607-620.

Chen, Y. L. L. (2000) Comparisons of primary productivity and phytoplankton size structure in the marginal regions of southern East China Sea. *Continental Shelf Res.*, 20: 437-458.

Chern, C.S. and J. Wang (1994) Influence of the seasonal thermocline on the intrusion of Kuroshio across the continental shelf northeast of Taiwan. *J. Oceanogr.*, 50: 691-711.

Denman, K. L. and M. R. Abbott (1994). Times scales of pattern evolution from cross-spectrum analysis of advanced very high resolution radiometer and coastal zone color scanner imagery. *J. Geogr. Res.*, 99: 7433-7442.

Fiedler, P. C. and H. J. Bernard (1987) Tuna aggregation and feeding near fronts observed in satellite imagery. *Continental Shelf Res.*, 7: 871-881.

Gong, G. C., J. Chang and Y. H. Wen (1999) Estimation of annual primary production in the Kuroshio waters northeast of Taiwan using a photosynthesis-irradiance model. *Deep-Sea Research I*, 46: 93-108.

Gong, G. C., F. K. Shiah, K. K. Liu, Y. H. Wen and M. H. Liang (2000) Spatial and temporal variation of chlorophyll *a*, primary productivity and chemical hydrography in the southern East China Sea. *Continental Shelf Res.*, 20: 411-436.

Hardman-Mountford N. J., A. J. Richardson, D. C. Boyer, A. Kreiner and H. J. Boyer (2003) Relating sardine recruitment in the Northern Benguela to satellite-derived sea surface height using a neural network pattern recognition approach. *Progress Oceanogr.*, 59: 241-255.

Hung, J. J., C. S. Lin, Y. C. Chung, G. W. Hung and W. S. Liu (2003) Lateral fluxes of biogenic particles through the Mien-Hua canyon in the southern East China Sea slope. *Continental Shelf Res.*, 23: 935-955.

Hur, H. B., G. A. Jacobs and W. J. Teague (1999) Monthly variations of water masses in the Yellow and East China Sea. *J. Oceanogr.*, 55: 171-184.

Hsueh, Y. (2000) The Kuroshio in the East China Sea. *J. Marine Syst.*, 24: 131-139.

Laurs, R. M., P. C. Fiedler and D. R. Montgomery (1984) Albacore tuna catch distributions relative to environmental features observed from satellites. *Deep Sea Res.*, 31: 1085-1099.

Li, Y. H. (1994). Material Exchange between the East China Sea and the Kuroshio Current. *Terrestrial, Atmos. Oceanic Sci.*, 5: 625-631.

Li, J. F. and Z. Chen (1998). Sediment resuspension and implications for turbidity maximum in the Changjiang Estuary. *Marine Geol.*, 148: 117-124.

Lin, C. Y., C. Z. Shyu and W. H. Shih (1992) The Kuroshio fronts and cold eddies off northeastern Taiwan observed by NOAA-AVHRR imageries. *Terrestrial, Atmos. Oceanic Sci.*, 3: 225-242.

Liu, K. K., G. C. Gong, S. Lin, C. Z. Shyu, S. C. Pai, C. L. Wei and S. Y. Chao (1992) Response of Kuroshio upwelling to the onset of northeast monsoon in the sea north of Taiwan: observations and a numerical simulation. *J. Geogr. Res.*, 97: 12511-12526.

Liu, Z. H., J. P. Xu and B. K. Zhu (2004). Observations of Argos satellite-tracked drifters in the Kuroshio area. *Donghai Marine Sci.*, 22: 1-10.

Lohrenz, S. E., G. L. Fahnenstiel, D. G. Redalje, G. A. Lang, M. J. Dagg, T. E. Whitledge and Q. Dortch (1999) Nutrients, irradiance, and mixing as factors regulating primary production in coastal waters impacted by the Mississippi River plume. *Continental Shelf Res.*, 19: 1113-1141.

McClain, E. P., W. G. Pichel and C. C. Walton (1985) Comparative performance of AVHRR-based multichannel sea surface temperature. *J. Geophys. Res.*, 90: 11587-11601.

Ning, X., Z. Liu, Y. Cai, M. Fang and F. Chai (1998) Physicobiological oceanographic remote sensing of the East China Sea: Satellite and in situ observations. *J. Geophys. Res.*, 103: 21623-21635.

Rodriguez, J. M., S. Hernandez-Leon and E. D. Barton (1999) Mesoscale distribution of fish larvae in relation to an upwelling filament off Northwest Africa. *Deep-Sea Res. I*, 46: 1969-1984.

Saitoh, S. I., D. Inagake, K. Sasaoka, J. Ishizaka, Y. Nakame and T. Saino (1998) Satellite and ship observations of Kuroshio warm-core ring 93A off Sanriku, northwestern North Pacific, in spring 1997. *J. Oceanogr.*, 54: 495-508.

SeaSpace (1992) TeraScan Reference Manual. San Diego, Calif. USA, 129pp.

Service, S. K., J. K. Rice and F. P. Chavez (1998) Relationship between physical and biological variables during the upwelling period in Monterey Bay, CA. Deep-Sea Res. II, 45: 1669-1685.

Shen, H. T., J. F. Li and H. F. Zhu (1993) Transport of the suspended sediment in the Changjiang Estuary. Intern. J. Sedimental Res., 7: 45-63.

Shi, F., X. L. Wang, X. Y. Shi, C. S. Zhang, F. H. Jiang, C. J. Zhu and K. Q. Li (2004) The benthic flux of dissolved nutrients at the sediment-water interface in the East China Sea. Marine Environ. Sci., 23: 5-8.

Sun, X. (1987) Analysis of surface path of the Kuroshio in the East China Sea. In Essays on the Investigation of Kuroshio, Ocean Press, Beijing, 1-14.

Sun, X. P. and S. M. Xiu (1997) Analysis on the cold eddies in the sea area northeast of Taiwan. Marine Sci. Bull., 16: 1-10.

Tang, T. Y. and W. T. Tang (1994). Current on the edge of the continental shelf northeast of Taiwan. Terrestrial, Atmos. Oceanic Sci., 5: 335-348.

Tang, T. Y., J. H. Tai and Y. J. Yang (2000) The flow pattern north of Taiwan and the migration of the Kuroshio. Continental Shelf Res., 20: 349-371.

Toba, Y. and H. Murakami (1998) Unusual behavior of the Kuroshio Current system from winter 1996 to summer 1997 revealed by ADEOS-OCTS and other data-suggestion of topographically forced alternating-jet instability. J. Oceanogr., 54: 465-478.

Tseng, C. T., C. Y. Lin, S.C. Chen and C. Z. Shyu (2000) Temporal and spatial variations of sea surface temperature in the East China Sea. Continental Shelf Res., 20: 373-387.

Wong, G. T. F., S. Y. Chao, Y. H. Li, F. K. Shiah (2000) The Kuroshio edge exchange processes (KEEP) study-an introduction to hypotheses and highlights. Continental Shelf Res., 20: 335-347.

Wong, G. T. F. and L. S. Zhang (2003) Geochemical dynamics of iodine in marginal seas: the southern East China Sea. Deep-Sea Res. (Part II, Topical Studies in Oceanography), 50: 1147-1162.

Wong, G. T. F., C. C. Hung and G. C. Gong (2004) Dissolved iodine species in the East China Sea-a complementary tracer for upwelling water on the shelf. Continental Shelf Res., 24: 1465-1484.

Yu, H. H. and Y. T. Miao (1990) Distribution Characteristic of thermocline near the continental slope in the East China Sea in summer 1987. In Essays on the investigation of Kuroshio(2), Ocean Press, Beijing, 136-144.

應用衛星遙測及水文觀測資料於東海海域黑潮湧昇現象之研究

曾振德^{1,2*}・孫志陸²・葉素然²・陳世欽¹・劉燈城³・蘇偉成³

¹行政院農業委員會水產試驗所企劃資訊組

²國立臺灣大學海洋研究所

³行政院農業委員會水產試驗所

摘要

本研究利用 NOAA 衛星 AVHRR 海面水溫影像、OrbView-2 衛星 SeaWiFS 海洋水色影像及現場水文調查資料等，綜合分析夏季時期的黑潮次表層水，於入侵東海南部陸棚區時，所形成的湧昇現象（冷渦分佈）及其發展過程。由連續的衛星水溫水色影像分析結果，顯示東海陸棚區的冷渦分佈型態及其涵蓋面積大小，均與船測的現場水文資料分析結果，具有顯著一致性。其中，分析 SeaWiFS 衛星海洋水色影像，發現黑潮湧昇區的海水葉綠素 a 濃度高於其周邊海域，平均值為 $0.61 \sim 1.31 \text{ mg/m}^3$ 。同時分析 AVHRR 衛星海面水溫影像，得知黑潮湧昇區的平均海面水溫為 19 至 21 度。此外，由現場 CTD 水文觀測資料分析結果，顯示出東海南部海域內的最高葉綠素 a 濃度，發生於彭佳嶼西方海域的黑潮湧昇區，約水下 35 m 處，其葉綠素 a 濃度可高達 1.99 mg/m^3 。且東海南部海域之次表層葉綠素 a 最大濃度分佈層則發生於 10 ~ 60 m 水深，然而於黑潮湧昇區，受海水自底層向上湧昇過程，其高濃度葉綠素 a 海水經常會擴展至 30 m 以淺的表層海域。綜合本研究分析結果，顯示利用衛星遙測獲得之海面水溫及海洋水色影像，確實可提供作為許多重要表層水文特徵（如黑潮湧昇現象及冷渦分佈等）之相關研究與分析。

關鍵詞：黑潮湧昇、冷渦、海面水溫、海洋水色

*通訊作者 / 基隆市和一路 199 號，TEL: (02) 2462-2101; FAX: (02) 2462-4627; e-mail: cttseng@mail.tfrin.gov.tw